DOI: 10.1002/chem.201001362

Quantification of CH···π Interactions: Implications on How Substituent Effects Influence Aromatic Interactions

Benjamin W. Gung,*[a] Bright U. Emenike,[a] Michael Lewis,[b] and Kristin Kirschbaum[c]

Abstract: Attractive interactions between a substituted benzene ring and an α-substituted acetate group were determined experimentally by using the triptycene model system. The attractive interaction correlates well with the Hammett constants σ_m ($R^2 = 0.90$), but correlates much better with the acidity of the α-protons ($R^2 = 0.98$).

Keywords: aromatic interactions · computational chemistry · Hammett plots · substituent effects · triptycenes

Introduction

Noncovalent interactions play an increasingly important role in modern chemical research.[1–3] Understanding the mechanisms involved in noncovalent interactions is important for the design of new supramolecular systems and biomolecular active agents.[4] Theoretical models of noncovalent interactions have been constantly evolving and in general the approach has been to partition intermolecular interactions into several fundamental physical forces.[5,6] A scheme by Hobza and Müller-Dethlefs partitioned noncovalent interaction energy into five components: 1) electrostatic, 2) charge-transfer, 3) dispersion, 4) ion-mediated, and 5) hydrophobic interactions.[6] Compared with Morokuma's original proposal,[5] electrostatic and charge-transfer interactions remained as fundamental forces in the scheme, while dispersion was added as an explicit term.[6]

The magnitudes of individual nonbonded interactions involving aromatic rings are provided mainly from high-level computational studies.[7–14] For the simple system of benzene dimers in the gas phase, the relative configurations from most to least stable in one of the more recent studies are calculated to be 1) parallel displaced (-2.74 kcal mol^{-1}), 2) edge-to-face (-2.39 kcal mol^{-1}), and 3) face-to-face stacked (-1.99 kcal mol^{-1}) (Figure 1).[11]

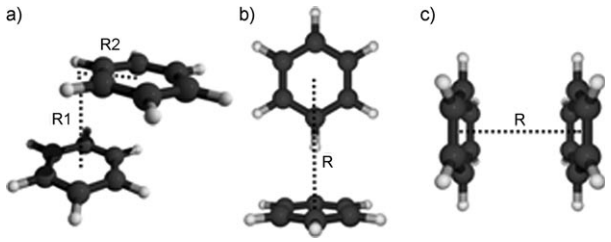

Figure 1. The orientations of interacting benzene dimer: a) parallel displaced, b) edge to face, and c) face to face.[11]

The first theoretical construct that specifically deals with aromatic interactions was proposed in 1990 by Hunter and Sanders.[15] This model is based on electrostatic interactions that describe the aromatic ring as a positively charged σ framework sandwiched between two regions of negatively charged π-electron density.[15] The hydrogen atoms carry partial positive charges and the π orbital carries partial negative charge. This model successfully explains the preferred arrangements between aromatic rings with a direct and effective electrostatic argument. Experimental studies using the 1,8-diarylnaphthalene system by Cozzi et al. support the theoretical construct of the Hunter and Sanders model.[16,17] Hobza and Müller-Dethlefs recently pointed out that it is enough to recognize the role of molecular quadrupoles in aromatic molecules for electrostatic arguments.[6] Although the simple electrostatic model for aromatic interactions has

[a] Prof. Dr. B. W. Gung, B. U. Emenike
Department of Chemistry and Biochemistry, Miami University
Oxford, Ohio 45056 (USA)
Fax: (+1) 513-529-5715
E-mail: gungbw@muohio.edu

[b] Prof. Dr. M. Lewis
Department of Chemistry, Saint Louis University
Saint Louis, MO 63103 (USA)

[c] Prof. Dr. K. Kirschbaum
Department of Chemistry, University of Toledo
Toledo, Ohio 43606 (USA)

Supporting information for this article is available on the WWW under http://dx.doi.org/10.1002/chem.201001362.

enjoyed acceptance for more than a decade, recent computational studies have raised the importance of dispersion forces and indicated that simple electrostatic models do not seem capable of explaining the energetic ordering of aromatic dimers with different substituents.[18] In general, Diederich et al. reported that experimental studies have emphasized electrostatic forces, whereas computational studies have emphasized dispersion forces.[2]

Along this line of debate, Wheeler and Houk have recently challenged the conventional concept of substituent effects in aromatic interactions based on a simple computational model.[19,20] It was suggested that substituents influence aromatic stacking interactions by interacting directly with another aromatic ring, rather than through the polarization of the arene. The computational results for substituent effects gave similar Hammett plots for a benzene dimer model and a simplified model system, despite the fact that the simple model system was devoid of an aromatic ring (Scheme 1). The results led to the conclusion that the substituent interacts directly with the other aromatic ring as indicated by the dashed lines between the substituent and the benzene ring in Scheme 1.[19]

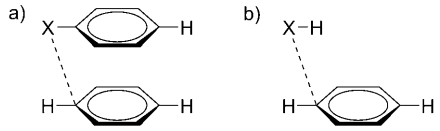

Scheme 1. Theoretical models used by Wheeler and Houk. a) Sandwich benzene dimer with one benzene ring with a substituent; b) the model that replaces the aromatic ring with a hydrogen atom. Both systems produced similar Hammett plots.

The traditional concept of π–π interactions tuned by substituents through electron withdrawal or donation to the aromatic rings was suggested to be flawed. Previously, Rashkin and Waters also described an unexpected direct interaction between substituents and the other aromatic ring.[21] However, they gave no generalized extrapolation to other systems. In a more recent theoretical study, Ringer and Sherrill have reported that simple models that account for only one type of interaction cannot capture the complexity of substituent effects.[22] The understanding of how substituents influence π–π interactions is important in drug design and in related fields.[2] We have prepared model systems attempting to reproduce the direct interactions between substituents and the other aromatic ring in solution. Our initial experimental results related to the direct interaction model were reported recently although no clear conclusion was reached.[23] Our further experimental results with model compounds **2a–g** and **3a–g** show a surprisingly linear correlation between calculated α-CH deprotonation energy and the *syn*/*anti* ratios. This correlation indicates a predominant CH···π interaction, rather than an X···π interaction as indicated in Scheme 1.[19] Further examination of the simplified model suggests that a dominant molecular dipole should place a partial positive charge on the hydrogen in the molecular fragment X–H. Thus, the results from this model study appear to represent more of an X–H···π interaction, rather than an X···π interaction.

Results and Discussion

The 1,9-disubstituted triptycene system has been demonstrated to be a valuable tool in our examination of arene–arene interactions, **1a–g** (Scheme 2).[24–26] The slow rotation of the C9 benzyl group around the C_{sp^3}–C_{sp^3} bond gives rise to *syn* and *anti* conformations, which can be studied by ^{1}H NMR spectroscopy (Scheme 3 and the Supporting Information). A statistical 2:1 *syn*/*anti* ratio is expected when there is no interaction between the C1 and the C9 groups. Because the triptycene scaffold provides an otherwise identical environment for the *syn* and *anti* conformations, any deviation from the statistical 2:1 *syn*/*anti* ratio indicates the

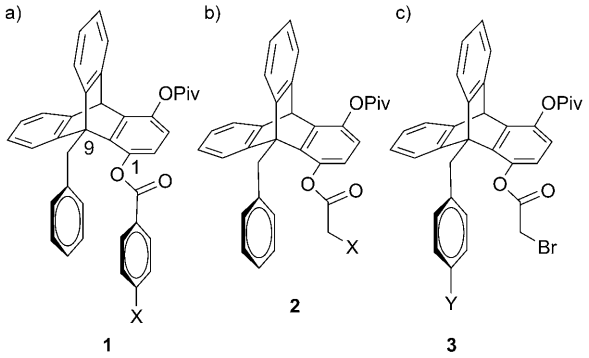

Scheme 2. a) The triptycene model **1a–g** have been established in the study of π–π interactions; b), c) the new models **2a–g** and **3a–g** were synthesized for studying direct interactions between the substituent X and the aromatic ring. Piv = pivaloyl; X = Me (**a**), OMe (**b**), H (**c**), Cl (**d**), Br (**e**), I (**f**), CN (**g**); Y = Me (**a**), H (**b**), F (**c**), Cl (**d**), Br (**e**), CN (**f**), NO_2 (**g**).

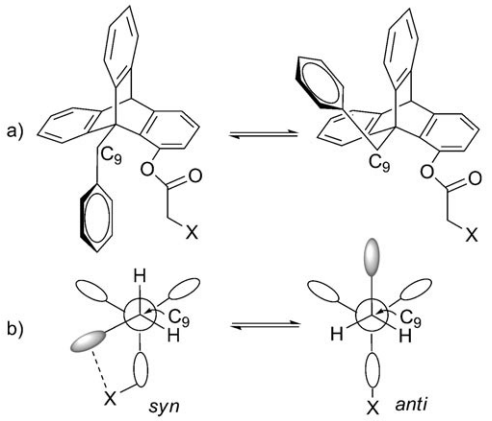

Scheme 3. a) Sketches to show the equilibrium between the *syn* and *anti* conformations. b) Newman projections at C9 show the diastereotopic protons in the *syn* conformation and the enantiotopic protons in the *anti* conformation, respectively.

degree of preference for the interactions between the C1 and the C9 groups. In this study, we replaced the C1 benzoate in previously used model system **1** with α-substituted acetates and correlated the *syn*/*anti* ratios obtained from the new models (**2a–g**, in which the substituent X is on the α-substituted acetate group, and **3a–g**, in which the substituent Y is on the C9 aromatic ring; Scheme 2) with Hammett constants σ_m and with the calculated deprotonation energy.

From the optimized conformations generated by MacroModel using the force field MMFFs, the distance between the substituent X and the C9 aromatic ring is 4.1 Å for the new model (**2d**, X = Cl; see Figure 2b) and 5.6 Å for the previous model (**1d**, not shown). Therefore, direct interactions between the substituent X and the C9 aromatic ring should be better reflected in the new models (**2a–g**).

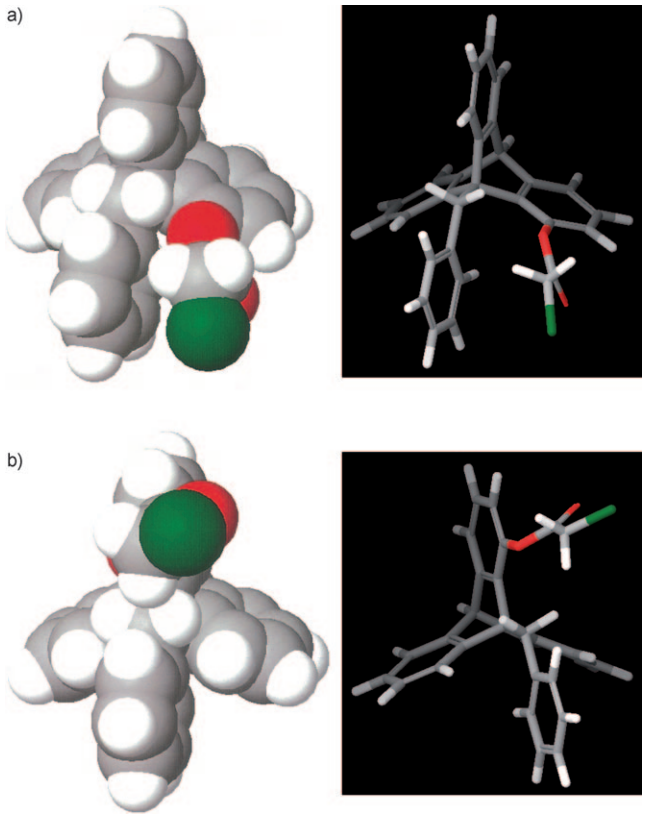

Figure 2. *syn* and *anti* conformations found by computer modeling (MacroModel 9.0, MMFFs force field) for compound **2d**.

The new series of triptycene compounds (**2a–g** and **3a–g**) were synthesized starting from the intermediates **4a–g**, previously reported for the synthesis of model compounds **1a–g**.[26] Commercially available acid chlorides were used whenever possible. In situ generation of acid chloride was employed when the corresponding acid was available (Scheme 4).

The *syn* conformation shows two sets of AB quartets in the ^{1}H NMR spectra at temperatures below −20 °C, which is illustrated in Figure 3 using compound **2d**. The signal for

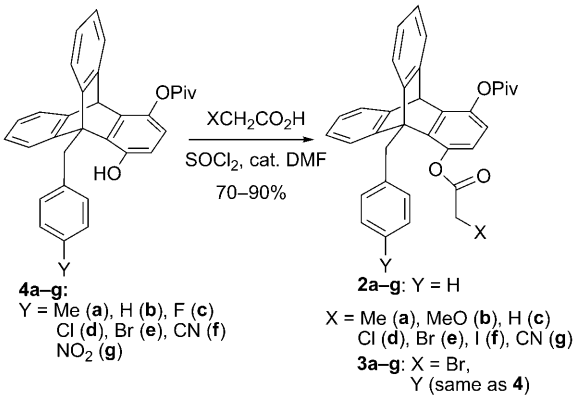

Scheme 4. Synthesis of the model compounds.

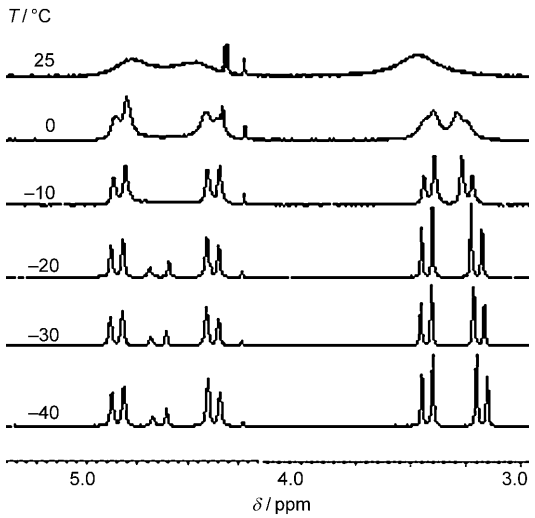

Figure 3. Temperature-dependent ^{1}H NMR (300 MHz) spectra for the C9 benzyl and CH_2Cl protons of model compound **2d**.

the benzyl CH_2 group appears centered at around δ = 4.6 ppm and the CH_2Cl group of compound **2d** appears at around δ = 3.3 ppm. The corresponding ^{1}H NMR signals for the *anti* conformation appear at around δ = 4.6 ppm as two small singlets, one from the benzyl and the other from the CH_2Cl group. This difference in chemical shifts for the CH_2Cl group between the *syn* and the *anti* conformation is an indication that the *syn* conformation places the CH_2Cl group in the "shielded" zone of the C9 aromatic ring, therefore, consistent with the proposed conformations.

A crystal suitable for X-ray structure analysis was obtained for model compound **3e** (Figure 4). The *syn* conformation is also preferred in the solid state and is similar to the optimized structures by MacroModel (Figure 2). The C–Br bond eclipses the carbonyl C=O bond, as shown in the X-ray structure. This arrangement allows the Br substituent to locate in the near van der Waals distance to assume a direct interaction with the aromatic ring of the benzyl

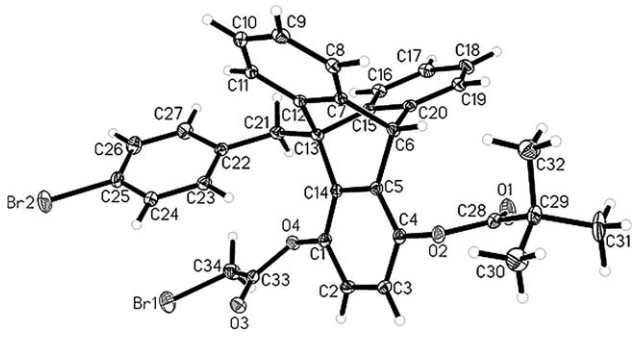

Figure 4. X-ray structure of compound **3e**. The *syn* conformation is also preferred in the solid state with a parallel stacking arrangement between the C9 arene and the C1 bromoacetate group. The nearest α-CH···arene distance is around 3.0 Å and α-Br···arene is around 4.0 Å.

group. Additionally, the α-CH proton is also close enough to interact with the aromatic ring.

The experimentally observed *syn*/*anti* ratios for compounds **2a**–**g** and **3a**–**g** and the corresponding free energies (calculated by using the equation: $\Delta G = -RT\ln K_{eq} = -RT\ln(1/2{\cdot}syn/anti\ \text{ratio})$) are compiled in Table 1. Elec-

Table 1. The ratios of *syn*/*anti* isomers for model compounds **2a**–**g** and **3a**–**g** (experiments were performed in $CDCl_3$).

Compound	Y	X	*syn*/*anti* ratio (−40 °C)	ΔG[a] [kcal mol^{-1}]
2c	H	H	3.7	−0.27
2a	H	Me	3.6	−0.26
2d	H	Cl	14.0	−0.86
2e	H	Br	11.2	−0.76
2f	H	I	10.6	−0.74
2b	H	OMe	7.4	−0.58
2g	H	CN	93.5	−1.70
3a	Me	Br	9.9	−0.73
3c	F	Br	6.2	−0.52
3d	Cl	Br	6.2	−0.52
3e	Br	Br	6.7	−0.54
3f	CN	Br	4.1	−0.33
3g	NO_2	Br	3.5	−0.24

[a] Errors are estimated at ±0.05 kcal mol^{-1} (from an average of two runs).

tron-withdrawing groups increase the *syn*/*anti* ratios for model compounds **2a**–**g**, in which the substituent is on the α-substituted acetate group. The *syn* conformation is favored for all compounds even though steric repulsions are possible in the *syn* arrangement. The highest *syn*/*anti* ratio is observed for compound **2g**, in which X = CN. The results are consistent with a CH···π interaction in which electron-withdrawing groups increase the acidity of the CH group, which in turn increases the attractive interaction.

The opposite is true for model compounds **3a**–**g**, that is, electron-withdrawing groups decrease the *syn*/*anti* ratios. Keep in mind that the substituent is on the C9 aromatic ring for **3a**–**g**, in which an electron-withdrawing group would reduce the π-electron density. Compounds **3a** and **3b**, in which Y = Me and H, show the highest *syn*/*anti* ratio, whereas **3g**, in which Y = NO_2, displays the lowest preference for the *syn* conformation. These observations are easy to explain with an X–H···π interaction, namely, there is less attraction when the aromatic ring is electron deficient. But it is difficult to rationalize with an X···π interaction. Because electron-withdrawing groups reduce the π-electron density of the aromatic ring in **3** and increase the acidity of the α-CH in **2**, the observed trend for the two series of model compounds suggests a predominant CH···π interaction.[27]

One way to verify this hypothesis is to correlate the interaction free energy with the acidity of the α-CH protons in compounds **2a**–**g**. We were not able to find any reported data on the acidity of α-substituted acetates and decided to carry out a set of ab initio calculations.[28] The deprotonation energy values for model compounds **2a**–**g** were obtained by calculations at the MP2(full)/6-311++G** level (except the iodo atom, which was calculated by using MIDIX) with Equation (1).[29]

$$\Delta E = E\ (\text{ester}) - E\ (\text{enolate}) \qquad (1)$$

The calculated energies related to acidity trend is given in Table 2. An increase in acidity corresponds to a decreasing value of ΔE. The acidity trends obtained for the α-substituted methyl acetates are $MeCH_2CO_2Me \approx HCH_2CO_2Me < MeOCH_2CO_2Me < ClCH_2CO_2Me \approx ICH_2CO_2Me \approx BrCH_2CO_2Me \ll CNCH_2CO_2Me$.

Table 2. Calculated deprotonation energies of **2a**–**g** at the MP2(full)/6-311++G**.[a]

Entry	X	*E* (ester) [a.u.]	*E* (enolate) [a.u.]	ΔE [kcal mol^{-1}]
1	Me	−307.0550875	−306.4436839	383.7
2	MeO	−382.1218883	−381.5179183	379.0
3	H	−267.8400638	−267.2296513	383.0
4	Cl	−726.9390650	−726.3452216	372.6
5	Br	−2840.133197	−2839.5422679	370.8
6	I	−7154.372297	−7153.7804367	371.4
7	CN	−359.9050864	−359.3485631	349.2

[a] The calculations were performed by using Gaussian 03.[28]

Once the interaction free energies and the acidity trends were collected, the data were analyzed through correlation with Hammett constants σ_m and with calculated deprotonation energy values ΔE. The results are shown in Figure 5.

The free energies determined at −40 °C from the *syn*/*anti* ratios were plotted against Hammett constants σ_m for compounds **3a**–**g** as shown in Figure 5a. Compounds **3a**–**g** have a fixed α-CH_2Br group linked to C1 acetate and a variable Y group on the C9 benzyl group. As the substituent Y becomes a stronger electron-withdrawing group, the attractive interactions diminish. A linear free energy relationship with $R^2 = 0.97$ was obtained. This is consistent with a predominant CH···π interaction. As the π-electron density of the aromatic ring decreases, the CH···π interaction also decreases. An alternative explanation would invoke direct Y···Br interactions because the distance between the substituent Y and the bromo atom is close enough to have a repulsive interaction in the *syn* conformation. However, the fact that the at-

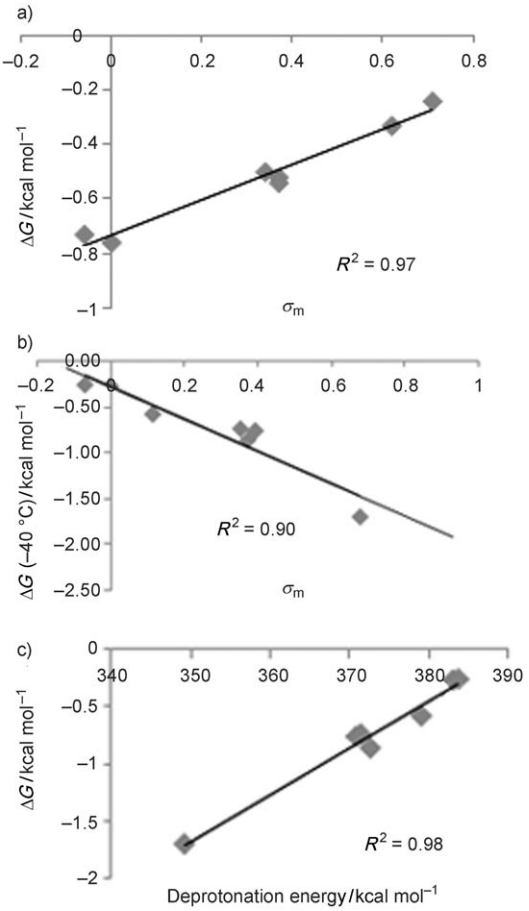

Figure 5. a), b) Plots of free energies versus Hammett constants σ_m and c) free energies versus calculated deprotonation energies, where a) is for **3a–g**, b) is for **2a–g**, and c) is for **2a–g**.

tractions decrease with an increasingly electron-deficient aromatic ring is inconsistent with an X(Br)···π interaction.

The *syn*/*anti* ratios for model compounds **2a–g** vary from 3.6 to 93.5 when X changes from methyl to CN (see Scheme 2 and Table 1). Compounds **2a–g** have a fixed C9 benzyl group with various substituent X attached to the α-carbon of the C1 acetate group. When X is a stronger electron-withdrawing group the *syn*/*anti* ratio increases rapidly. This trend does not rule out a direct interaction between the X group and the aromatic ring. However, it further supports the notion that an attractive CH···π interaction is predominant in the *syn* conformations. Thus, an electron-withdrawing group increases the acidity of the α-CH protons, which in turn enhances the attractive CH···π interaction. To verify that this is indeed the case, two correlations are made: one uses Hammett constants (Figure 5b) and the other uses the deprotonation energy (Figure 5c).

The free energies determined at −40 °C from the *syn*/*anti* ratios are plotted against Hammett constants σ_m for compounds **2a–g** as shown in Figure 5b. A linear free energy relationship with $R^2 = 0.90$ was obtained. This is consistent with the fact that σ_m is a good indicator of the electron-withdrawing ability of the substituent. However, the correlation is not nearly as good as when the substituent is on the benzene ring, such as in compounds **3a–g** (Figure 5a).

The free energies determined at −40 °C from the *syn*/*anti* ratios were also plotted against the calculated deprotonation energies in the gas phase (Figure 5c). An excellent linear correlation with $R^2 = 0.98$ was obtained. This is by far the strongest support for the predominance of the CH···π interactions in the *syn* conformation of **2a–g**. The Hammett constants σ_m give an excellent correlation for compounds **3a–g** when the substituent is on the aromatic ring (Figure 5a) as they should be. However, they also provide a fairly straight line as in Figure 5b even though the substituent is not on an aromatic ring. Our experimental results from model compounds **2a–g** and **3a–g** made us reexamine the results reported by Wheeler and Houk.[19] It appears that an attenuated (due to the computational constraint placed on the distance between the XH and the benzene ring) X–H···π interaction has been captured by the simple model. As shown in Scheme 1b, the partially positive hydrogen atom of the X–H group is pointed near the negative π system of the benzene ring. The X–H···π interaction appears to have resulted in the similar Hammett plots obtained in the original report.[19]

Conclusion

Our experimental study has shown that a predominant CH···π interaction controls the conformational preference of model compounds **2a–g** and **3a–g**. Despite the predominance of the CH···π interaction in compounds **2a–g**, a Hammett plot displays a fairly straight line for the substituent effect. These results show that when using Hammett plots in a simplified model system one should be mindful of the limitations. We initially set out to identify the proposed X···π interactions, but we are now convinced that the predominant interactions are of the CH···π type in **2a–g** and **3a–g**. The model compounds **2a–g** and **3a–g** cannot exclude the CH···π interactions from X···π interactions. Therefore they are not ideal model compounds to study X···π interactions. However, the same can be said about the simple model shown in Scheme 1b. The benzene dimer is a prototype system for studying aromatic interactions and extensive theoretical studies have been reported on such systems.[30] The replacement of one benzene ring in a benzene dimer system with a hydrogen atom went one step further in simplifying real world aromatic interactions. We caution against using such simplifications when examining arene–arene interactions, since our experimental results have shown that misleading conclusions may be obtained. Instead, computational studies should explore more realistic systems of aromatic interactions and avoid generalization from studies of a simplified model system.

Experimental Section

Representative procedure for the preparation of the model compounds 9-Phenyl-1-propionyl-4-trimethylacetyloxytriptycene (2a): Compound **4a** (100 mg, 0.208 mmol) was added to a solution of 4-dimethylaminopyridine (DMAP; 5.3 mg, 0.042 mmol), pyridine (0.5 mL, 10.5 mmol), and CH_2Cl_2 (2 mL) under a nitrogen atmosphere. After stirring the mixture for 10 min at 0°C, propionyl chloride (29 mg, 0.313 mmol) was added by syringe. The reaction was monitored by TLC. After completion, the reaction was warmed to room temperature, diluted with CH_2Cl_2, and quenched with 1 N HCl. The aqueous layer was extracted three times with Et_2O, and the combined organic extracts were washed with a 10% aqueous solution of NaOH and brine. The organic extracts were dried over $MgSO_4$, filtered, concentrated, and purified by silica gel flash chromatography (5→10→20% EtOAc/hexanes) to yield a white solid (87 mg, 78%). M.p. 238–240°C; ^{1}H NMR (500 MHz, $CDCl_3$): $\delta = 0.99$–1.01 (br s, 3H), 1.61 (s, 9H), 2.02–2.20 (br s, 2H), 4.68 (br s, 2H), 5.54 (s, 1H), 6.78–7.39 ppm (m, 15H); ^{13}C NMR (125 MHz, $CDCl_3$): $\delta = 27.5$, 34.7, 39.5, 48.7, 52.8, 119.8, 121.4, 123.7, 124.9, 125.6, 137.9, 129.7, 142.9, 143.9, 172.3, 176.5 ppm; LCMS: m/z: 539.3

Variable-temperature NMR spectroscopy experimental procedure: The ^{1}H NMR spectra were recorded on a 300 MHz instrument with a variable-temperature probe. A 0.03 M solution of the sample in a deuterated solvent, such as chloroform, was placed in a high-quality NMR tube. All samples were degassed by using a needle to bubble nitrogen through the sample for about 1 min. The NMR tube was then capped and sealed with parafilm. The sample tube was placed into the NMR probe and the airline to the probe was replaced with liquid-nitrogen transfer line. The desired temperature was set on the variable-temperature unit and the sample was allowed to equilibrate for 10–15 min at each set temperature. Then the ^{1}H NMR spectrum at each temperature was recorded. The ratios of rotamers were obtained through the integrations of selected peaks.

Acknowledgements

B.W.G. thanks the CFR of Miami University for a summer stipend. M.L. thanks the National Center for Supercomputing Applications (CHE050039N) for time on the Dell Intel 64 Linux Cluster. We thank Laura K. E. Hardebeck and Selina Wireduaah for technical assistance with the ab initio computations.

[1] J. M. Lehn, *Supramolecular Chemistry: Concepts and Perspectives*, VCH, Weinheim, **1995**, p. 271.
[2] E. A. Meyer, R. K. Castellano, F. Diederich, *Angew. Chem.* **2003**, *115*, 1244–1287; *Angew. Chem. Int. Ed.* **2003**, *42*, 1210–1250.
[3] J. Cerny, P. Hobza, *Phys. Chem. Chem. Phys.* **2007**, *9*, 5291–5303.
[4] H. J. Schneider, *Angew. Chem.* **2009**, *121*, 3982–4036; *Angew. Chem. Int. Ed.* **2009**, *48*, 3924–3977.
[5] K. Morokuma, *Acc. Chem. Res.* **1977**, *10*, 294–300.
[6] K. Müller-Dethlefs, P. Hobza, *Chem. Rev.* **2000**, *100*, 143–167.
[7] W. L. Jorgensen, D. L. Severance, *J. Am. Chem. Soc.* **1990**, *112*, 4768–4774.
[8] G. D. Smith, R. L. Jaffe, *J. Phys. Chem.* **1996**, *100*, 9624–9630.
[9] P. Hobza, H. L. Selzle, E. W. Schlag, *J. Phys. Chem.* **1996**, *100*, 18790–18794.
[10] R. L. Jaffe, G. D. Smith, *J. Chem. Phys.* **1996**, *105*, 2780–2788.
[11] M. O. Sinnokrot, E. F. Valeev, C. D. Sherrill, *J. Am. Chem. Soc.* **2002**, *124*, 10887–10893.
[12] F. Tran, J. Weber, T. A. Wesolowski, *Helv. Chim. Acta* **2001**, *84*, 1489–1503.
[13] S. Tsuzuki, K. Honda, T. Uchimaru, M. Mikami, K. Tanabe, *J. Am. Chem. Soc.* **2002**, *124*, 104–112.
[14] E. C. Lee, B. H. Hong, J. Y. Lee, J. C. Kim, D. Kim, Y. Kim, P. Tarakeshwar, K. S. Kim, *J. Am. Chem. Soc.* **2005**, *127*, 4530–4537.
[15] C. A. Hunter, J. K. M. Sanders, *J. Am. Chem. Soc.* **1990**, *112*, 5525–5534.
[16] F. Cozzi, M. Cinquini, R. Annuziata, J. S. Siegel, *J. Am. Chem. Soc.* **1993**, *115*, 5330–5331.
[17] F. Cozzi, M. Cinquini, R. Annunziata, T. Dwyer, J. S. Siegel, *J. Am. Chem. Soc.* **1992**, *114*, 5729–5733.
[18] M. O. Sinnokrot, C. D. Sherrill, *J. Am. Chem. Soc.* **2004**, *126*, 7690–7697.
[19] S. E. Wheeler, K. N. Houk, *J. Am. Chem. Soc.* **2008**, *130*, 10854.
[20] S. E. Wheeler, K. N. Houk, *J. Am. Chem. Soc.* **2009**, *131*, 3126.
[21] M. J. Rashkin, M. L. Waters, *J. Am. Chem. Soc.* **2002**, *124*, 1860–1861.
[22] A. L. Ringer, C. D. Sherrill, *J. Am. Chem. Soc.* **2009**, *131*, 4574.
[23] B. W. Gung, B. U. Emenike, C. N. Alverez, J. Rakovan, K. Kirschbaum, N. Jain, *Tetrahedron Lett.* **2010**, *51*, 1648–1650.
[24] B. W. Gung, F. Wekesa, C. L. Barnes, *J. Org. Chem.* **2008**, *73*, 1803–1808.
[25] B. W. Gung, M. Patel, X. W. Xue, *J. Org. Chem.* **2005**, *70*, 10532–10537.
[26] B. W. Gung, X. W. Xue, H. J. Reich, *J. Org. Chem.* **2005**, *70*, 3641–3644.
[27] M. Nishio, M. Hirota and Y. Umezawa, *The CH/pi Interaction: Evidence, Nature and Consequences*, Wiley-VCH, Weinheim, **1998**.
[28] Gaussian 03, Revision C.02, M. J. Frisch, G. W. Trucks, H. B. Schlegel, G. E. Scuseria, M. A. Robb, J. R. Cheeseman, J. A. Montgomery, Jr., T. Vreven, K. N. Kudin, J. C. Burant, J. M. Millam, S. S. Iyengar, J. Tomasi, V. Barone, B. Mennucci, M. Cossi, G. Scalmani, N. Rega, G. A. Petersson, H. Nakatsuji, M. Hada, M. Ehara, K. Toyota, R. Fukuda, J. Hasegawa, M. Ishida, T. Nakajima, Y. Honda, O. Kitao, H. Nakai, M. Klene, X. Li, J. E. Knox, H. P. Hratchian, J. B. Cross, V. Bakken, C. Adamo, J. Jaramillo, R. Gomperts, R. E. Stratmann, O. Yazyev, A. J. Austin, R. Cammi, C. Pomelli, J. W. Ochterski, P. Y. Ayala, K. Morokuma, G. A. Voth, P. Salvador, J. J. Dannenberg, V. G. Zakrzewski, S. Dapprich, A. D. Daniels, M. C. Strain, O. Farkas, D. K. Malick, A. D. Rabuck, K. Raghavachari, J. B. Foresman, J. V. Ortiz, Q. Cui, A. G. Baboul, S. Clifford, J. Cioslowski, B. B. Stefanov, G. Liu, A. Liashenko, P. Piskorz, I. Komaromi, R. L. Martin, D. J. Fox, T. Keith, M. A. Al-Laham, C. Y. Peng, A. Nanayakkara, M. Challacombe, P. M. W. Gill, B. Johnson, W. Chen, M. W. Wong, C. Gonzalez, J. A. Pople, Gaussian, Inc., Wallingford CT, **2004**.
[29] S. Damoun, W. Langenaeker, G. Vandewoude, P. Geerlings, *J. Phys. Chem.* **1995**, *99*, 12151–12157.
[30] M. O. Sinnokrot, C. D. Sherrill, *J. Phys. Chem. A* **2006**, *110*, 10656–10668.

Received: May 18, 2010
Published online: September 17, 2010

